





CORRELATING DEPOSITION PARAMETERS WITH STRUCTURE AND PROPERTIES OF NANOSCALE MULTILAYER (TiSi)N/CrN COATINGS[†]

 Vyacheslav M. Beresnev^a,  Olga V. Maksakova^a,  Serhiy V. Lytovchenko^{a*},
 Serhiy A. Klymenko^b,  Denis V. Horokh^a,  Andrey S. Manohin^b,  Bohdan O. Mazilin^a,
 Volodymyr O. Chyshkala^a,  Vyacheslav A. Stolbovoy^c

^a*V.N. Karazin Kharkiv National University
4, Svobody Sq., 61000 Kharkiv, Ukraine*

^b*V.M. Bakula Institute of Superhard Materials of the National Academy of Sciences of Ukraine
2, Avtozavodska str., 04074 Kyiv, Ukraine*

^c*National Science Center «Kharkiv Institute of Physics and Technology»
1, Akademichna Str., 61108 Kharkiv, Ukraine*

Corresponding Author: s.lytovchenko@karazin.ua, (+380)-50-694-33-21

Received May 2, 2022; accepted May 30, 2022

Multilayer (TiSi)N/CrN coatings were fabricated through vacuum-arc deposition by applying the arc currents of (100 ÷ 110) A on TiSi cathode and (80 ÷ 90) A on Cr cathode, negative bias potential connected to the substrate holder of $-(100 \div 200)$ V and reactive gas pressure of (0.03 ÷ 0.6) Pa. Applying a negative bias voltage on substrates enhanced the ion bombardment effect, which affected the chemical compositions, phase state, mechanical and tribological properties of (TiSi)N/CrN coatings. Obtained results indicated that (TiSi)N/CrN coatings with Si content ranging from 0.53 to 1.02 at. % exhibited a high hardness level of (22.1 ÷ 31.1) GPa accompanied with a high Young's modulus of (209 ÷ 305) GPa, H/E* level of (0.080 ÷ 0.100), H³/E*² level of (0.15 ÷ 0.33) GPa, and the friction coefficient of 0.35. Values of critical loads at dynamic indentation, changes in friction coefficient and level of acoustic emission signal evidence the high adhesive strength of (TiSi)N/CrN coatings, which allows recommending them to increase cutting tool performance.

Keywords: multilayer coatings, refractory metal nitrides, hardness, adhesive strength

PACS: 61.46.-w, 62.20. Qp, 62-65.-g

INTRODUCTION

CrN-based coatings are well known for their higher ductility and fracture toughness, lower coefficient of friction, and excellent oxidation and corrosion resistance compared to extensively used TiN coatings [1, 2]. Additionally, the lower coefficients of friction of CrN coatings provide better wear resistance than TiN coatings under dry sliding conditions; in addition, their high toughness prevents the initiation and propagation of cracks in erosive environments. For these reasons, CrN coatings have been used to protect cutting tools in the machining of copper, aluminium, and titanium based alloys [3] and have become a successful alternative to TiN coatings for protecting injection moulding tools. However, in other potential industries, CrN coatings demonstrate limited use due to their relatively low hardness compared to TiN [3]. In recent years, almost all single-layer coatings satisfy the needs of industry less and less and do not always meet the requirements for increasing their performance. Nanocomposite coatings based on nitrides of the refractory metals are one of the prospective basements in the development of up-to-date multifunctional coatings as they have high both physical and mechanical properties. The combination of mentioned properties of known coatings based on nitrides and carbides of the refractory metals is achieved by their doping with such elements as Al, Si, B, etc. A good example of such doping is the Ti-Si-N ternary system with a silicon content of about 5~10 at.; it has high hardness (≥ 40 GPa) and better oxidation resistance compared to traditional TiN coatings [4, 5]. These characteristics are mainly explained by the structure of the film, which is defined as a nanocomposite consisting of nanocrystalline TiN embedded in amorphous Si₃N₄ [6–8]. In addition, the amorphous phase becomes an oxygen barrier that slows down the oxidation [8]. However, despite all the advantages of the nanocomposite structure, there is a high residual stress between the TiSiN film and the substrate, which causes low adhesion [9]. At the same time, CrN-based coatings are commonly used as a protective hard coating on tool steels for industrial applications due to its good adhesion strength, chemical stability, and high temperature oxidation resistance.

Therefore, in this study, CrN coatings are used as intermediate (second) layers for the formation of (TiSi)N/CrN periodic structure. Such a multilayer coating with layers of nanometer thickness makes it possible to achieve the better hardness and fracture toughness compared to single-layer coatings due to the interfaces that prevent the movement of dislocations and the difference in the elastic modulus of the layers.

EXPERIMENTAL DETAILS AND METHODS

Multilayer coatings were obtained by the vacuum-arc deposition technique. Two cathodes made of TiSi with the elemental composition of Ti = 94 at.% & Si = 6 at.% and hot-pressed Cr with a purity of about 99.6 % were used as

[†] **Cite as:** V.M. Beresnev, O.V. Maksakova, S.V. Lytovchenko, S.A. Klymenko, D.V. Horokh, A.S. Manohin, B.O. Mazilin, V.O. Chyshkala, and V.A. Stolbovoy, East Eur. J. Phys. 2, 112 (2022), <https://doi.org/10.26565/2312-4334-2022-2-14>

© V.M. Beresnev, O.V. Maksakova, S.V. Lytovchenko, S.A. Klymenko, D.V. Horokh, A.S. Manohin, B.O. Mazilin, V.O. Chyshkala, and V.A. Stolbovoy, 2022

evaporated materials. The regime of the deposition was a continuous rotation of the samples at a speed of 8 rpm. The total deposition time was 1.5 hours. The material of the substrate was an austenitic chromium-nickel stainless steel. The dimensions of the substrate were: length $L = 18$ mm, width $W = 18$ mm and thickness $H = 3$ mm. Four series of samples were formed at different pressures of the reaction gas ($P_N = 0.08 \div 0.6$ Pa) and bias potential ($U_b = -100 \div -200$ V). To manage the nanoscale diapason of the layers, the thickness of the deposited layers was estimated. The calculations were carried out on the basis of a theoretical model, which was described in [10]. When the deposition of a coating on a rotating substrate, during the evaporation, the surface of the substrates alternately passes through zones directly near the operating evaporators, and zones in which deposition on the substrate does not occur as a result of the action of geometrical factors. Therefore, a generalized solution was obtained for calculating the thickness of the deposited layers, including dependences on the size of the holder with samples r at a given radius R , as well as on the angle α , since the angular values in these zones and the rate of condensation at an arbitrary point will also change (see Fig. 1). In the case where condensation of the substance occurs on a single rotating surface located at a distance r from the axis of the chamber (corresponding to half the size of the sample holder), with two simultaneously operating evaporators on a circle with radius R (distance between cathode and samples), there are the following zones: "shadow" zone of space in which there is no condensation of the direct flow of the target cathode material; zones in which condensation of material that evaporates from only one evaporator occurs; as well as zones where the flows of materials from the two evaporators overlap to varying degrees (depending on r - the ratio r / R and α - the angle of rotation of the sample holder; at some values of r these zones are not realized).

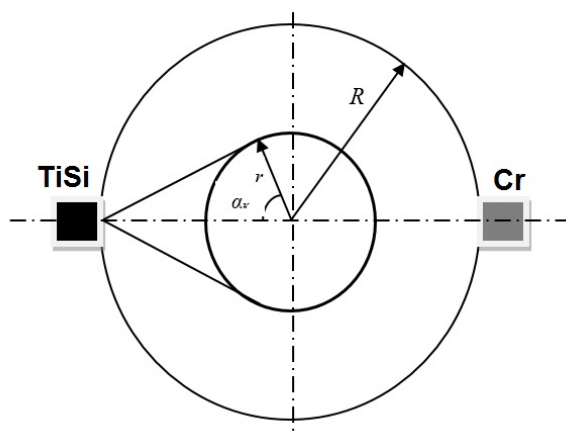


Figure 1. Scheme of deposition of multilayer (TiSi)N/CrN coatings from two evaporators (TiSi and Cr) on a rotating steel substrate.

Table 1 presents the results of calculating the deposition rates and thicknesses of the layers deposited during one rotation of the holder for multilayer (TiSi)N/CrN coatings (V_0 is the condensation rate of the material flow during a normal fall on a stationary substrate).

Table 1. Deposition rates of multilayer (TiSi)N/CrN coatings.

Evaporator	Radius R , mm	Size of the holder r , mm	r'	Angle α , deg	Rotation speed ω , rpm	V_0 , nm/s	Thickness after 1 rotation h_t , nm
TiSi	200	125	0,625	51	8	0,69	3,21
Cr						0,75	3,49

The physical and technological parameters, as well as the elemental composition of the obtained coatings, are shown in Table 2.

Table 2. Technological parameters and elemental composition of multilayer (TiSi)N/CrN coatings.

Seria	Coating	Arc current $I_{TiSi/I_{Cr}}$, A	Reaction gas P_N , Pa	Bias potential U_b , V	Elemental composition, at.%			
					Ti	Si	Cr	N
<i>a</i>	(TiSi)N/CrN	110/90	0.08	-100	52.05	0.89	21.13	25.93
<i>b</i>		100/80	0.08	-200	41.39	0.94	28.80	28.87
<i>c</i>		100/80	0.3	-200	38.54	1.02	17.40	43.04
<i>d</i>		100/80	0.6	-200	30.15	0.53	17.21	52.11

The study of elemental composition of the coatings was carried out by analyzing the spectra of characteristic X-ray radiation generated by an electron beam in a scanning electron microscope FEI Nova NanoSEM 450. The spectra were recorded using an EDAX PEGASUS energy-dispersive X-ray spectrometer fitted to a scanning electron microscope. Phase analysis was carried out by X-ray diffractometry in $Cu\text{-}\alpha$ radiation in a DRON-4 setup. The hardness of the coatings was measured using a high performance micro-hardness testing machine equipped with the

Vickers indenter. The load of 0.4903 N (50 g) was applied for a time of 10–15 s. Adhesion strength of the coatings was determined by sclerometry with simultaneous registration of acoustic emission (AE) signals. The Revetest scratch tester by CSM Instruments with a diamond spherical indenter of Rockwell C type with a radius of 200 microns was used to determine the adhesion characteristics.

RESULTS AND DISCUSSIONS

The results of the analysis of the elemental composition of the coatings (see Table 2) indicate that they consist of the elements of the cathodes, i.e. Ti, Si, Cr and N. With an increase in the bias potential, the amount of titanium and chromium decreases. Fig. 2 shows a cross-sectional image of multilayer (TiSi)N/CrN coating (seria c) obtained by the vacuum arc deposition.

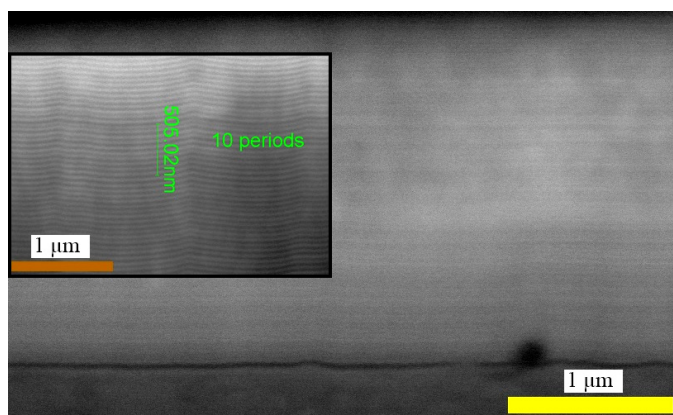


Figure 2. Cross-sectional image of multilayer (TiSi)N/CrN coating (seria c) obtained at $U_b = -200$ V and $P_N = 0.3$ Pa.

The low content of Si in the coating does not lead to the separation with the formation of the SiN_x phase [4], which is confirmed by the absence of peaks corresponding to this phase in diffraction spectra (see Fig. 3).

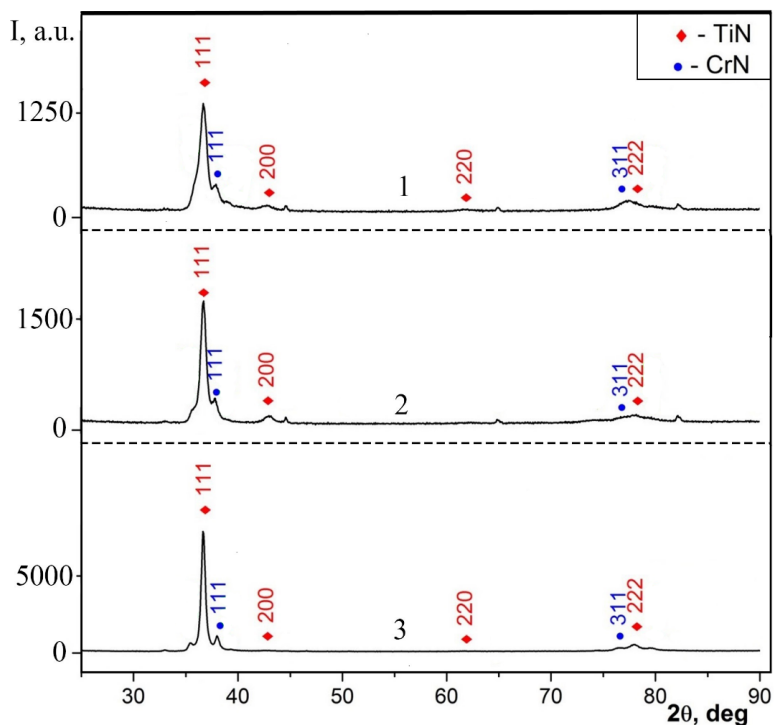


Figure 3. XRD spectra of multilayer (TiSi)N/CrN coatings obtained at $U_b = -200$ V and $P_N = 0.08$ Pa (spectrum 1), $P_N = 0.3$ Pa (spectrum 2) Pa, $P_N = 0.6$ Pa (spectrum 3).

As expected, the nitrogen content is minimal (in the case of the coatings obtained at the lowest gas pressure of 0.08 Pa); therefore, as the analysis of X-ray diffraction spectra (see Fig. 3) has shown, it manifests itself in a bound form, which is characterized by the formation of two phases with strong nitride-forming titanium (with dissolved silicon), forming Ti(Si)N nitride with the preferred orientation of crystallites along the [111] axis and chromium nitride CrN with the [111] axis (see Fig. 3. spectra 1). The calculated lattice periods are 0.4244 nm of (TiSi)N and 0.4101 nm of CrN, and the corresponding sizes of the crystallites are 24.1 nm ((TiSi)N) and 26.8 nm (CrN), respectively.

The spectra also show the presence of α -Ti and Cr phases, where the nitrogen content is so low that the formation of Ti and/or Cr nitride phases becomes impossible. With an increase in the nitrogen pressure to 0.6 Pa, the coating maintains the [111] texture. The lattice period of TiN decreases to 0.4240 nm, while lattice period of CrN increases to 0.4109 nm. The structure of the coating becomes more fine-grained as the crystallite size of TiN and CrN decreases to 12.9 nm and 13.7 nm, respectively (see Fig. 3 spectrum 3). The separation of (111)TiN and (111)CrN diffraction lines indicates the presence of a strong homogeneous [111] texture in both nitride layers. Thus, when forming the coating with sufficiently thin layers (about 7 nm), a significantly higher heat of formation of titanium nitride (see Table 3) leads to a redistribution of nitrogen atoms at low pressure (0.08 ÷ 0.3 Pa), during deposition from Cr to Ti layers (the process is also enhanced by the presence in these Si layers), which is accompanied by the formation of TiSiN and CrN. And only at a high pressure of 0.6 Pa, when TiN is saturated, the separate TiN and CrN phases are formed.

Table 3. Enthalpies of formation (ΔH) of binary metal nitrides and silicides based on studied elements [11, 12].

Enthalpy of formation ΔH , kJ/mol	TiN	TiSi ₂	Si ₃ N ₄	CrN	CrSi ₂
	-337,7	-171,0	-750	-123,2	-77,4

It is known that, in addition to hardness H and reduced Young's modulus E^* , the important characteristics of the coating functionality, that assess the fracture toughness, are the elastic strain to failure and the resistance to plastic deformation, which are presented by the ratios of H/E^* and H^3/E^{*2} , respectively. The H^3/E^{*2} ratio determines the level of toughness of the coating. At the same time, the H/E^* ratio makes it possible to evaluate the deformation of the contacting surfaces [13, 14]. The results of the calculations of H , E^* , H/E^* и H^3/E^{*2} ratios of multilayer (TiSi)N/CrN coatings are presented in Table 4.

Table 4. Mechanical characteristics of multilayer (TiSi)N/CrN coatings

Seria	Reaction gas P_N , Pa	Bias potential U_b , V	Hardness H , GPa	Young's modulus E^* , GPa	H/E^*	H^3/E^{*2}
<i>a</i>	0.08	-100	22.1	209	0.1	0.22
<i>b</i>	0.08	-200	24.5	305	0.08	0.15
<i>c</i>	0.3	-200	28.2	275	0.1	0.28
<i>d</i>	0.6	-200	31.1	298	0.1	0.33

The calculated H/E^* and H^3/E^{*2} ratios for all obtained coatings demonstrate the highest values of the resistance to plastic deformation ($H/E^* > 0.1$ according to the hard nanocomposite films categorization generalized by Musil et al.). The higher level of H^3/E^{*2} , the better resistance of the coating to the formation and propagation of cracks. It should be noted that the maximum hardness value of 31.1 GPa is identified for multilayer (TiSi)N/CrN coating seria *d* obtained at $P_N = 0.6$ Pa and $U_b = -200$ V, which is characterized by rather low crystallite sizes (12.9 nm for (TiSi)N and 13.7 nm for CrN layers), as well as by the best-developed growth texture [111]. From the structural engineering point of view, this state corresponds to the presence of nitride phases (TiSi)N and CrN with an isostructural crystal lattice of the NaCl type in both layers. It should also be noted that layers with lower hardness (CrN) prevent the propagation of cracks in hard layers ((TiSi)N) when operating under dynamic loads, since softer chromium nitride layers have high fracture toughness and resistance to deformation, which makes them promising for use as wear resistant coatings.

To determine the adhesive strength, scratches were applied to the surface of the coatings under progressive loading on the indenter from 0.9 N to 190 N. According to [15], depending on various values of critical loads, several physicochemical processes occur simultaneously during abrasion, however, only L_C is directly related to adhesive failure.

Fig. 4 shows the image of a scratch on the surface of multilayer (TiSi)N/CrN coating seria *d* obtained at $P_N = 0.6$ Pa and $U_b = -200$ V, as well as the change in the average values of the friction coefficient μ (left scale) and the acoustic emission amplitude AE (right scale).

The following main critical loads were recorded by changing the curves of the dependence of the friction coefficient and acoustic emission on the load: L_{C1} is the moment of appearance of the first chevron crack at the bottom and a diagonal crack along the edges of the scratch; L_{C2} is the moment of appearance of chevron cracks at the bottom of the scratch; L_{C3} is the moment of the formation of many chevron cracks at the bottom of the scratch and local peeling of the coating; L_{C4} is the moment of appearance of cohesive-adhesive destructions of the coating; L_{C5} is the moment of plastic abrasion of the coating to the substrate.

To compare the obtained results, the adhesion characteristics of single-layer (TiSi)N and CrN coatings obtained under the same conditions as multilayer (TiSi)N/CrN coatings were used. An analysis of scratches on the surface of (TiSi)N/CrN indicates that the appearance of fluctuations in the acoustic emission signal at low loads is associated not with the destruction of the coating, but with the presence of defects on its surface and structure. When the load increases to 28,9 H (see Table 5, load L_{C3}) the formation of chipping occurs along the edges of the scratch. It is confirmed by a slight increase in the amplitude of acoustic emission and the coefficient of friction; moreover, it increases the penetration depth of the indenter. Obtained results indicate that during scratching multilayer (TiSi)N/CrN coatings wear

out, but do not exfoliate; thus, they are destroyed by the cohesive mechanism associated with plastic deformation and the formation of fatigue cracks in the structure of the coating.

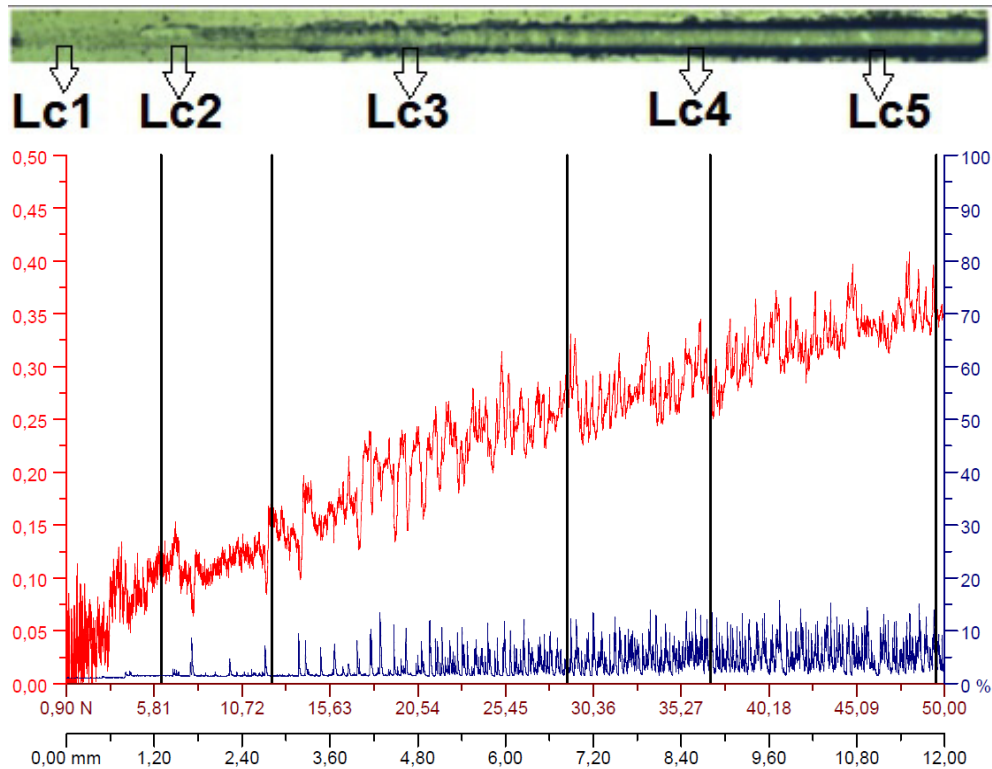


Figure 4. Image of a scratch on the surface of multilayer (TiSi)N/CrN coating obtained at $P_N = 0.6$ Pa and $U_b = -200$ V, as well as the change in the average values of the friction coefficient μ (left scale, red line) and the acoustic emission amplitude AE (right scale, blue line) along the scratch.

Initially, the surface of the coating resists the penetration of the indenter. In this case, the friction coefficient increases non-monotonically, while the amplitude AE signal changes insignificantly (see Fig. 4). Further, with an increase in the load, chips and solely flakes appear along the edges of the scratch (see Fig. 4, image of the scratch); the penetration depth of the indenter continues to increase. The formation of such cracks is accompanied by an increase in the amplitude of acoustic emission and the coefficient of friction. The appearance of the substrate material at the bottom of the scratch is noted when the load L_{C5} reaches 49.54 N (see Fig. 4 and Table 5).

Table 5. Comparative results of the adhesion testing of multilayer (TiSi)N/CrN coating (seria *d*) and single-layer (TiSi)N and CrN coatings










Coating	Reaction gas P_N , Pa	Bias potential U_b , V	Load, N					Friction coefficient, μ
			L_{C1}	L_{C2}	L_{C3}	L_{C4}	L_{C5}	
(TiSi)N/CrN	0.6	-200	6.1	12.4	28.9	36.8	49.5	0.35
(TiSi)N	0.6	-100	9.5	12.4	18.3	48.8	45.3	0.55
CrN	0.6	-100	4.5	7.8	12.3	25.5	37.5	0.24

CONCLUSIONS

1. The effect of vacuum-arc deposition parameters on the composition, structure, and properties of multilayer (TiSi)N/CrN coatings has been studied. It is shown that the two-phase system of NaCl-type structure (fcc crystal lattice) is formed in both nitride layers. The preferred orientation for all obtained coatings is (111).
2. It has been established that in multilayer (TiSi)N/CrN coatings, the nanolayered periodic structure of the layers is even, flat and does not contain visible defects. The smallest crystallites size is 12.9 nm for (TiSi)N and 13.7 nm for CrN layers. Such a nanoscale structure provides the maximum value of hardness of 31.1 GPa and Young's modulus of 298 GPa. The main difference in the structure and properties of multilayer coatings is primarily due to differences in the energy impact of Ti, Si Cr ions on the radiation-stimulated processes of coating formation.
3. The adhesion strength of multilayer (TiSi)N/CrN coating is higher by 10 % compared to single-layer (TiSi)N and/or CrN coatings. The nanoscale multilayer structure decreases the friction mechanisms, i.e. the friction coefficient of (TiSi)N/CrN coating is 0.35, while for (TiSi)N is 0.55.

This research was supported by the National Research Foundation of Ukraine (Grant No. 2020.02/0234).

ORCID IDs

-  Vyacheslav M. Beresnev, <https://orcid.org/0000-0002-4623-3243>;  Olga V. Maksakova, <https://orcid.org/0000-0002-0646-6704>
 Serhiy V. Lytovchenko, <https://orcid.org/0000-0002-3292-5468>;  Serhiy A. Klymenko, <https://orcid.org/0000-0003-1464-3771>
 Denis V. Horokh, <https://orcid.org/0000-0002-6222-4574>;  Andrey S. Manohin, <https://orcid.org/0000-0003-1479-8482>
 Bohdan O. Mazilin, <https://orcid.org/0000-0003-1576-0590>;  Volodymyr O. Chyshkala, <https://orcid.org/0000-0002-8634-4212>
 Vyacheslav A. Stolbovoy, <https://orcid.org/0000-0001-7734-0642>

REFERENCES

- [1] F. Cai, X. Huang, Q. Yang, R. Wie, and D. Nagy. Surf. and Coat. Technol. **205**, 182 (2010), <https://doi.org/10.1016/j.surfcoat.2010.06.033>
- [2] A.O. Andreev, L.P. Sablev, and S.N. Grigor'ev, *Вакуумно-дуговые покрытия* [Vacuum-arc coatings] (Kharkiv, NNC KIPT, 2010), pp. (in Russian).
- [3] B. Navinšek, P. Panjan, and I. Milošev. Surf. and Coat. Technol. **97**(1-3), 182 (1997), [https://doi.org/10.1016/S0257-8972\(97\)00393-9](https://doi.org/10.1016/S0257-8972(97)00393-9)
- [4] S. Veprek, M. Veprek-Heijman, P. Karvankova, and O. Prochazka, Thin Solid Films. **476**(1), 1-29 (2005), <https://doi.org/10.1016/j.tsf.2004.10.053>
- [5] A.D. Pogrebnyak, A.P. Shpak, N.A. Azarenkov, and V.M. Beresnev, Physics-Uspekhi, **52**(1), 29 (2009), <https://doi.org/10.3367/UFNe.0179.200901b.0035>
- [6] H. Zeman, J. Musil, and P. Zeman, J. Vac. Sci. Technol. **A22**(3), 646-664 (2004).
- [7] P.J. Martin, A. Bendavid, J.M. Cairney, and M. Hoffman, Surf. and Coat. Technol. **200**(7), 2228-2235 (2005), <https://doi.org/10.1016/j.surfcoat.2004.06.012>
- [8] A. Cavaleiro, and J. Hosson, *Nanostructured Coatings* (Springer New York, NY, 2006), pp. 648, <https://doi.org/10.1007/978-0-387-48756-4>
- [9] Sh.-Min Yang, Yi.-Yu.Chang, D.-Yi.Lin, Da-Yu.Wang, and W. Wu, Surf. & Coat. Technol. **202**(10), 2176 (2008), <https://doi.org/10.1016/j.surfcoat.2007.09.004>
- [10] Y.V. Kunchenko, V.V. Kunchenko, I.M. Neklyudov, G.N. Kartmazov, and A.A. Andreev, PAST, **2**(90), 203 (2007), https://vant.kipt.kharkov.ua/ARTICLE/VANT_2007_2/article_2007_2_203.pdf
- [11] G.V. Samsonov and I.M. Vinnitskiy, *Тугоплавкие соединения: справочник* [Refractory compounds: handbook] (Metallurgiya, Moscow, 1976), 560 p. (in Russian).
- [12] G.V. Samsonov, L.A. Dvorina, and P.V. Rud', *Силициды* [Silicides] (Metallurgiya, Moscow, 1979), pp. 272. (in Russian).
- [13] S.A. Firstov, V.F. Gorban', E.P. Pechkovskiy, and N.A. Mameka, Materialovedenie, **11**, 26 (2007).
- [14] D.V. Shtansky, S.A. Kulnich, E.A. Levashov, A.N. Sheveiko, F.V. Kirihancev, and J.J. Moore, Thin Solid Films. **420-421**, 330 (2002), [https://doi.org/10.1016/S0040-6090\(02\)00942-2](https://doi.org/10.1016/S0040-6090(02)00942-2)
- [15] J. Valli, J. Vac. Sci. Technol. A, **4**, 3007 (1986) <https://doi.org/10.1116/1.573616>

**КОРЕЛЯЦІЯ МІЖ ПАРАМЕТРАМИ ОСАДЖЕННЯ ТА СТРУКТУРОЮ І ВЛАСТИВОСТЯМИ
НАНОРОЗМІРНИХ БАГАТОШАРОВИХ ПОКРИТТІВ (TiSi)N/CrN**

**В.М. Береснев^а, О.В. Максакова^а, С.В. Литовченко^а, С.А. Клименко^б, Д.В. Горох^а, А.С. Манохін^б,
Б.О. Мазілін^а, В.О. Чишкала^а, В.О. Столбовой^с,**

^а*Харківський національний університет імені В.Н. Каразіна, майдан Свободи 4, 61022, м. Харків, Україна*

^б*Інститут надтвердих матеріалів ім. В.М. Бакуля НАН України, вул. Автозаводська, 2, 04074, м. Київ, Україна*

^с*Національний науковий центр «Харківський фізико-технічний інститут», вул. Академічна, 1, 61108, м. Харків, Україна*

Багатошарові покриття (TiSi)N/CrN сформовані методом вакуумно-дугового осадження з двох катодів при струмах дуги (100 ÷ 110) А на TiSi катоді і (80 ÷ 90) А на Cr катоді. Негативний потенціал зміщення на тримачі підкладки становив (100 ÷ 200) В, а тиск реактивного газу в камері (0,03 ÷ 0,6) Па. Негативний потенціал зміщення на підкладках посилював дію іонного бомбардування, що вплинуло на хімічний склад, фазовий стан, механічні та трибологічні властивості покриттів (TiSi)N/CrN. Отримані результати показали, що покриття (TiSi)N/CrN з вмістом Si від 0,53 до 1,02 ат.% мають високу твердість (22,1 ÷ 31,1) ГПа разом з високим модулем Юнга (209 ÷ 305) ГПа, рівнем Н/Е* (0,080 ÷ 0,100), рівнем Н³/Е*² (0,15 ÷ 0, 33) ГПа та коефіцієнтом тертя 0,35. Значення критичних навантажень при динамічному вдавлюванні, зміни коефіцієнта тертя і рівня сигналу акустичної емісії при склерометрії свідчать про високу адгезійну міцність покриттів (TiSi)N/CrN, що є підставою рекомендувати їх для підвищення продуктивності різального інструменту.

Ключові слова: багатошарові покриття, нітриди тугоплавких металів, твердість, адгезійна міцність.